Available online at www.sciencedirect.com
ScienceDirect
Carbohydrate Polymers 73 (2008) 44–54
Carbohydrate Polymers
www.elsevier.com/locate/carbpol

Chitosan nanoparticles loaded with dorzolamide and pramipexole

Sofia Papadimitriou [a], Dimitrios Bikiaris [a,*], Konstantinos Avgoustakis [b], Evangelos Karavas [c], Manolis Georgarakis [d]

[a] *Laboratory of Organic Chemical Technology, Department of Chemistry, Aristotle University of Thessaloniki, 541 24 Thessaloniki, Greece*
[b] *Laboratory of Pharmaceutical Technology, Department of Pharmacy, University of Patras, Rio 26500, Patras, Greece*
[c] *Pharmathen S.A., Pharmaceutical Industry, Dervenakion Str., 6, Pallini Attikis, 153 51 Attiki, Greece*
[d] *Section of Pharmaceutics and Drug Control, Department of Pharmacy, Aristotle University of Thessaloniki, 541 24 Thessaloniki, Greece*

Received 25 June 2007; received in revised form 16 October 2007; accepted 2 November 2007
Available online 13 November 2007

Abstract

Chitosan (CS) nanoparticles of dorzolamide hydrochloride (Dorzo) and pramipexole hydrochloride (Prami) were prepared by the ionic gelation method and their in vitro properties were studied. The long-term objective is the development of efficient ocular formulations for Dorzo and efficient oral formulations for Prami. The particle size of nanoparticles was affected by the CS/drug ratio whereas it was not affected by the type of drug (Dorzo or Prami). Drug association efficiency to the nanoparticles did not appear to correlate with the drug/CS ratio whereas the loading capacity tended to fall with increasing drug proportion. Based on WAXD data, Dorzo was dispersed in the nanoparticles in crystalline form, probably due to the weak interaction developed between Dorzo and CS/TPP matrix as FT-IR data indicated. In contrast, WAXD and step-scan DSC data indicated that Prami formed a molecular dispersion within the nanoparticles. This was probably due to the potent interactions developed between Prami and CS/TPP matrix, as FT-IR data revealed. The nanoparticles exhibited mucoadhesive properties which diminished with increasing drug content. Sustained in vitro drug release was observed with the Dorzo-loaded CS nanoparticles in PBS (pH 7.4) and with the Prami-loaded CS nanoparticles in simulated intestinal fluid. The results obtained in this study suggest that the Dorzo-loaded CS nanoparticles and the Prami-loaded CS nanoparticles could be further evaluated for the controlled ocular delivery of Dorzo and the controlled oral delivery of Prami, respectively.
© 2007 Elsevier Ltd. All rights reserved.

Keywords: Chitosan; Nanoparticles; Ionotropic gelation; Pramipexole; Dorzolamide

1. Introduction

CS, a (1-4)2-amino 2-deoxy β-D-glucan, is a deacetylated form of chitin, an abundant polysaccharide present in crustacean shells. CS is biocompatible (Hirano & Noishiki, 1985) and, because of its cationic nature, has good mucoadhesive and membrane permeability-enhancing properties (Illum, 1998, 2007). Therefore, CS has been extensively investigated for its potential as absorption enhancer across intestinal epithelium for drugs, peptides, and proteins (Kotez et al., 1997; Lavelle, 2000; Takeuchi, Yamamoto, Niwa, Hino, & Kawashima, 1996; Van der Lubben, Verhoef, Borchard, & Junginer, 2001) and for the preparation of various systems for mucosal drug delivery (Cui, Qian, & Yin, 2006; Dodane & Vilivalam, 1998; Kumar, Muzzarelli, Muzzarelli, Sashiwa, & Domb, 2004; Paul & Sharma, 2000; Prego, Garcia, Torres, & Alonso, 2005). Hydrophilic nanoparticles based on CS receive currently increasing interest as they could control the rate of drug release, prolonging the duration of the therapeutic effect, and deliver the drug to specific sites in the body (Agnihotri, Mallikarjuna, & Aminabhavi, 2004; Janes, Calvo, & Alonso, 2001; Prabaharan & Mano, 2005). CS can form nanoparticles using, amongst other methods, ionotropic gelation. The method is based on the gelation of CS when it comes in contact with specific polyanions due to the formation of inter- and intramolecular cross-linkages mediated by these poly-

* Corresponding author. Tel.: +30 2310 997812; fax: +30 2310 997667.
E-mail address: dbic@chem.auth.gr (D. Bikiaris).

0144-8617/$ - see front matter © 2007 Elsevier Ltd. All rights reserved.
doi:10.1016/j.carbpol.2007.11.007

anions (Janes et al., 2001). Bodmeier et al. was the first to report the inotropic gelation of CS with tripolyphosphate (TPP) for drug encapsulation (Bodmeier, Chen, & Paeratakul, 1989) while Alonso et al. developed CS nanoparticles with the addition of a solution containing TPP into an acidic phase (pH 4–6) containing CS (Alonso, Calvo, Remunan, & Vila-Jato, 2001; Calvo, Remunan-Lopez, Vila-Jato, & Alonso, 1997). The study of Wu et al. showed that the formation of nanoparticles is only possible within specific, moderate concentrations of CS and TPP (Wu, Yang, Wang, Hu, & Fu, 2005). Furthermore, the CS/TPP weight ratio should be within the range of 4:1–6:1 in order to obtain a high yield of nanoparticles (Zhang, Oh, Allen, & Kumacheva, 2004). Ionic cross-linking of CS with TPP represents an advantageous method of preparation of drug-loaded nanoparticles, since it is an extremely mild process yielding nanoparticles of controllable size (from 200 nm up to 1 μm) and satisfactory encapsulation capacity for drugs and macromolecules like proteins, peptides and oligonucleotides (Janes et al., 2001).

In the present study, CS nanoparticles of Dorzo and Prami were prepared and their in vitro properties were studied (Scheme 1). Our long-term objective is the development of efficient ocular formulations for Dorzo and efficient oral formulations for Prami. Dorzo is a carbonic anhydrase inhibitor used for decreasing aqueous humour secretion in the ciliary processes of the eye. The topical administration of Dorzo in the front part of the eye with conventional pharmaceutical preparations (e.g. eye drops) is inefficient since, after application, these preparations are diluted rapidly with tears and are discharged through the lachrymal duct. Ocular administration of Dorzo in the form of mucoadhesive CS nanoparticles can be expected to increase the time of drug residence on eye surface, increasing drug bioavailability and prolonging the pharmacological effect. Prami is a novel dopamine agonist indicated for treatment of the signs and symptoms of idiopathic Parkinson's disease. It is administered as Prami in three equal oral doses per day, and the daily dose should be carefully titrated to maximize therapeutic effect and reduce the incidence and severity of side effects. Incorporation of Prami in a controlled release system, such as the CS nanoparticles, could provide for a more efficient control of drug levels in blood, reducing side-effects and, by decreasing the frequency of administration, could improve patient compliance.

2. Experimental

2.1. Materials

CS with high molecular weight was supplied from Aldrich chemicals (MW: 350,000 g/mol, deacetylation degree >75% and viscosity 800–2000 cps), TPP was supplied by Aldrich chemicals. Prami was purchased from Amino Chemicals Ltd. (Malta) (assay 99.2%) and Dorzo was purchased from Regactives (Boecielo Valladolid, Spain) (assay 99.3%). All other materials and reagents used in this study were of analytical grade of purity.

2.2. Preparation of CS nanoparticles

CS nanoparticles were prepared according to the ionotropic gelation method (Calvo et al., 1997). Blank nanopar-

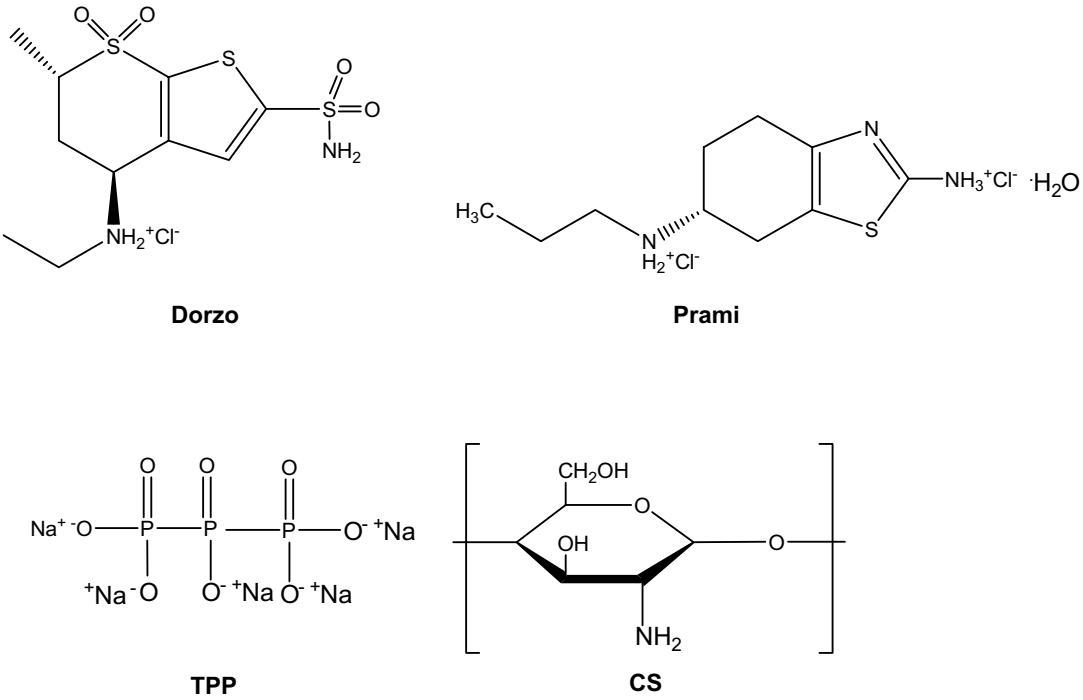

Scheme 1. Molecular structures of Dorzo, Prami, TPP and CS.

ticles were obtained upon the addition of TPP aqueous solution (final concentrations 0.5, 2 mg/ml, respectively) to a CS acetic acid solution. Different concentrations of CS and TPP were used in order to determine the CS/TPP ratios providing nanoparticles with optimum size properties (CS/TPP ratios 1/2, 1/4, 1/5, final concentrations always 2 mg/mL and for TPP 1, 0.5 and 0.4 mg/mL, respectively). The concentration of acetic acid was in all cases 1.75 times higher than that of CS. The formation of nanoparticles was a result, as previously reported (Aktas et al., 2005) of the interaction between the negative groups of TPP and the positively charged amino groups of CS. For the preparation of drug-loaded nanoparticles, Prami or Dorzo aqueous solutions were added in the CS solution. Three different drug concentrations were used, 10%, 25% and 50% (w/w) of drug based on CS, in order to study the effect of the drug loading on the morphological and physicochemical characteristics of nanoparticles as well as on the in vitro release properties. Every sample was prepared in triplicate and the results represent the average value. Non-entrapped drug was removed by ultracentifugation at 30,000*g* for 45 min at 4 °C and resuspension of the pellet in pure water. The purified nanoparticles were freeze-dried.

2.3. Characterization of CS nanoparticles

2.3.1. Morphological characterization of nanoparticles

Transmission electron microscopy (TEM) was used to examine the morphology of the nanoparticles prepared in this study. TEM micrographs of nanoparticle samples deposited on copper grids were obtained with a JEOL 120 CX microscope (Japan), operating at 120 kV.

2.3.2. Size measurements of nanoparticles

The particle size distribution of CS/drug nanoparticles was determined by dynamic light scattering (DLS) using a Zetasizer Nano Instrument (Malvern Instruments, Nano ZS, ZEN3600, UK) operating with a 532 nm laser. A suitable amount of nanoparticles was dispersed in distilled water creating a total concentration 1‰ and was kept at 37 °C under agitation at 100 rpm.

2.3.3. Wide angle X-Ray diffractometry (WAXD)

WAXD was used to investigate the physical form (crystalline or amorphous) of drug dispersion within the CS matrix of the nanoparticles. The WAXD experiments were performed over the range 2θ from 5 to 50 °C, using a Philips PW 1710 diffractometer with Bragg-Brentano geometry $(\theta, 2\theta)$ and Ni-filtered CuKa radiation.

2.3.4. Differential scanning calorimetry

DSC study was performed on a Perkin-Elmer Pyris 1 DSC, equipped with Intracooler 2P cooling accessory. Accurately weighed nanoparticle samples (5 mg) were placed in standard aluminium pans and sealed with a lid. Heating rates of 20 °C/min were applied with a nitrogen purge of 20 mL/min. Also, Modulated-Temperature DSC (MTDSC) study was performed using the same instrument used for standard DSC analysis. The Step-Scan Software of Perkin-Elmer was used. Step-Scan DSC is a temperature modulated DSC technique that operates, in conjunction with the power compensation DSC. The approach applies a series of short heating and isothermal steps to cover the temperature range of interest. With the Step-Scan DSC approach, two signals are obtained. Thermodynamic C_p signal represents the reversible changes of the material, while the isothermal signal reflects the irreversible changes of the sample during heating. In this study heating steps of 4 °C at a heating rate 10 °C/min between isothermal steps of 0.4 min were selected. Thus, scans from 0 to 200 °C were performed and the average heating rate was 5 °C/min.

2.3.5. Fourier transformation-infrared spectroscopy (FT-IR)

FT-IR spectra were obtained using a Perkin-Elmer FT-IR spectrometer, model Spectrum 1000. In order to collect the spectra, a small amount of freeze-dried nanoparticles was mixed with KBr (1 wt% nanoparticles) and compressed to form tablets. The IR spectra of these tablets, in absorbance mode, were obtained in the spectral region of 450–4000 cm^{-1} using a resolution of 4 cm^{-1} and 64 co-added scans.

2.3.6. Evaluation of drug encapsulation

The drug-loaded nanoparticles were centrifuged as described in paragraph 2.2 and the amount of non-entrapped drug (free drug) was measured in the clear supernatant using UV spectrometry (Shimadzu PharmaSpec UV-1700). The corresponding calibration curves were produced using the supernatant of blank nanoparticles. Each sample was measured in triplicate. For Prami the calibration curve was created at 262 nm where the drug gives its characteristic peak while Dorzo shows a characteristic peak at 254 nm.

The drug loading capacity (LC) and association efficiency (AE) of the nanoparticles were calculated according to the following equations:

$$\%\mathrm{LC} = \frac{\text{Total drug-free drug}}{\text{Nanoparticle weight}} \times 100$$

$$\%\mathrm{AE} = \frac{\text{Total drug-free drug}}{\text{Total drug amount}} \times 100$$

2.4. Assessment of the mucoadhesive force

Two different methods were applied in order to estimate the adhesive force of the nanoparticles.

2.4.1. First method

The method described in the literature to estimate the number of mucoadhesive microspheres was used with

slight modifications (Kamath & Park, 1994). The CS nanoparticles were immersed in a 50 mL glass bicker at 37 °C containing a phosphate buffer solution (0.05 M, pH 7.4) for 5 min in such a way that the solution just covered the nanoparticles. After nanoparticles wetting, a round fresh pig intestinal mucosa (PIM) with a diameter similar to that of glass beaker was placed on nanoparticles surface so as to cover all the nanoparticles and remained for 5 min in contact with the nanoparticles. The intestinal mucosa with the attached nanoparticles was removed and the remaining nanoparticles on the glass beaker were dried at 60 °C till constant weight. The percent of adhered nanoparticles (AN) was estimated using the following equation:

$$\text{AN } (\%) = [(W_o - W_r)/W_o] \times 100$$

where W_o is the initial weight of nanoparticles and W_r the remained unattached weight of nanoparticles.

2.4.2. Second method (Yin, Chen, Qiao, Lu, & Hu, 2006)

The binding efficiency of mucin to nanoparticles was determined by mixing 1 mL of pig mucin (PM, Sigma) suspension in PBS (0.05 M, pH 7.4) with the same volume of nanoparticles. After incubation at 37 °C for 30 min, the samples were centrifuged (35000*g*, 20 min). The concentration of free PM in the supernatant was determined at 251 nm by UV spectrometry (Shimadzu PharmaSpec UV-1700). The PM binding efficiency of nanoparticles was calculated from the following equation:

$$\text{PM binding efficiency } (\%) = [(C_o - C_s)/C_o] \times 100$$

where C_o is the initial concentration of PM used for incubation, and C_s is the concentration of free PM in the supernatant.

2.5. In vitro drug release

Nanoparticle samples (1 mL), enclosed in dialysis bags (cellulose membrane, mw cut-off 12400, Sigma), were incubated in 40 mL release medium at 37 °C under mild agitation in a water bath. The release medium was simulated intestinal fluid (pH 7.4) or simulated gastric fluid (pH 1.2) in the case of Prami/CS nanoparticles and phosphate buffered saline (PBS, pH 7.4) in the case of Dorzo/CS nanoparticles At predetermined time intervals, 500 μl samples were withdrawn from the incubation medium and analyzed for drug (Dorzo or Prami) by UV spectrometry as described in the previous paragraph. After sampling, 500 μl of fresh medium were added in the incubation medium. Control experiments to determine the release behavior of the free drug was also performed. Dorzo and Prami hydrochloride were dissolved in PBS and simulated intestinal fluid respectively, and 1 mL of each solution ($c = 1$ mg/mL), enclosed in a dialysis bag, was immersed in 40 mL of the respective medium. Then, the procedure described above for the nanoparticle samples was followed.

3. Results and discussion

3.1. Size, morphology and drug loading properties of CS nanoparticles

CS nanoparticles can easily be prepared upon the incorporation of TPP solution to the CS solution under magnetic stirring, since the creation of nanoparticles depends mainly on the evolved ionic interaction of CS with TPP that eventually leads to the reduction of aqueous solubility of CS. The ratio between CS and TPP is critical and controls the size and the size distribution of the nanoparticles. The size characteristics have been found to affect the biological performance of CS nanoparticles (Pan et al., 2002). For this reason before the drug encapsulation into CS nanoparticles, the effect of CS/TPP ratio on the size characteristics of the nanoparticles was studied in order to find the optimum ratio that result to nanoparticles of low size and narrow size distribution. In Fig. 1 the particle size distribution for the different CS/TPP ratios, obtained by DLS, is presented.

It is clear that by increasing the CS/TPP ratio, nanoparticles with smaller sizes are produced. It appears that the optimum CS/TPP ratio among these studied here is 5/1 w/w, which might be related to the fact that TPP is a poly-functional cross-linking agent and can create five ionic cross-linking points with amino groups of CS. As a result, the CS/TPP 5/1 weight ratio lead to the most efficient cross-linking of amino groups producing the most compact particle structure (Zhang et al., 2004). At this ratio, CS nanoparticles with sizes less than 300 nm are produced (Fig. 1). Thus, this ratio was selected for the preparation of drug-loaded nanoparticles. With all CS/TPP ratios studied, bimodal size distributions were obtained in which, apart from the main peak, a low peak at small sizes (between 30 and 60 nm) appeared. The formation of a low fraction of nanoparticles having much smaller size than the main nanoparticles population may indicate the presence

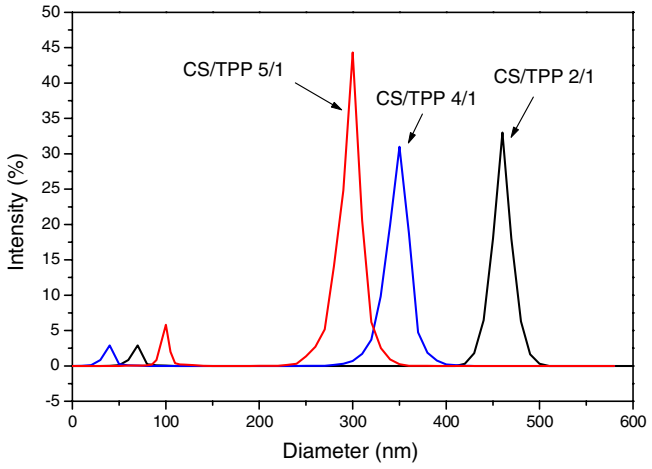

Fig. 1. Variation of particle size distribution using different CS/TPP ratios.

of low molecular weight fragments in commercially available CS. These smaller chains can form nanoparticles of lower size (Janes & Alonso, 2003).

The drug-loaded nanoparticles exhibited relatively narrow particle size distribution, as the relatively low polydispersity index (PDI) values of DLS measurements (Table 1) would indicate. The TEM images (Fig. 2) also indicated that CS/drug nanoparticles were roughly spherical in shape. The size of the nanoparticles based on the TEM micrographs was about 50–70 nm smaller than the size determined by DLS. This could have been expected since the nanoparticles were dispersed in an aqueous phase for the DLS experiments, and CS has the ability to swell in contact with water, while the TEM experiments were performed in dry samples (Aktas et al., 2005). The particle size of the drug-loaded nanoparticles was affected by the CS/drug ratio whereas it was not affected by the type of drug (Dorzo or Prami) (Table 1). It is obvious from Table 1 that the incorporation of drugs into CS nanoparticles leads to a drug proportion-dependent increase of their size compared with the blank (non-loaded) nanoparticles. This is in agreement with previously reported data (Fernandez-Urrusuno, Calvo, Remunan-Lopez, Vila-Jato, & Alonso, 1999; Kim et al., 2006) and may be attributed to the reduction of ionic interactions between CS and TPP during nanoparticles formation because of the presence of the drug molecules. Both drugs (Dorzo and Prami) are positively charged and can, in principle, develop ionic interactions with the negatively charged TPP ions or CS (these interactions as well as the drug interactions with CS were investigated with FT-IR, see next paragraph). Increasing drug proportion caused an increasing reduction of CS/TPP interaction, leading to increasing nanoparticles size (Table 1). When the drug/CS weight ratio increased from 10/90 to 50/50 w/w, the average size of CS/Prami nanoparticles was increased from 289 to 452 nm and the size of CS/Dorzo nanoparticles was increased from 300 to 443 nm (Table 1). Drug efficiency of the nanoparticles did not appear to correlate with the drug/CS ratio whereas the loading capacity tended to fall with increasing drug proportion (Table 1). With both drugs, favourable size and drug loading were obtained with the CS/drug weight ratio of 90/10 w/w (Table 1). It has been reported that the loading capacity of nanoparticles with drug depends on many factors, such as CS molecular weight, TPP content, CS concentration and drug concentration (Deng, Zhou, & Luo, 2006).

Table 1
Particle diameter and drug encapsulation of different weight ratios between CS and the used drugs

CS/Drug (w/w)	Nanoparticles diameter (nm)	PDI	AE (%)	LC (%)
CS/TPP	275 ± 6	0.51	–	–
CS/Prami 90/10	289 ± 6	0.451	29.1 ± 0.4	0.76 ± 0.014
CS/Prami 75/25	346 ± 9	0.425	18.9 ± 0.4	0.54 ± 0.008
CS/Prami 50/50	452 ± 1	0.492	21.4 ± 1.2	0.43 ± 0.023
CS/Dorzo 90/10	300 ± 5	0.616	17.8 ± 0.8	0.68 ± 0.032
CS/Dorzo 75/25	349 ± 6	0.458	17.9 ± 0.7	0.46 ± 0.016
CS/Dorzo 50/50	443 ± 4	0.531	19.6 ± 1.4	0.54 ± 0.025

3.2. Interaction between the encapsulated drugs and nanoparticle's matrix

The nature of interactions between the drugs and CS or TPP was established with FT-IR spectroscopy since any kind of physicochemical interaction that may take place, like the formation of hydrogen bonds between the drugs and CS or TPP, will automatically lead to frequency shifts or splitting in absorption peaks. In the slightly acidic aqueous medium, where nanoparticles formation occurs, both drugs will be positively charged because of the existence of primary and secondary amino groups in their molecular structure (Fig. 3). As a result, the electrostatic interaction between the drug molecules and TPP can be included, besides hydrogen bonding, in the possible interaction mechanisms between the drug and nanoparticles' matrix (CS).

Several characteristic absorbances can be identified in the FT-IR spectrum of pure CS (Fig. 4). At 3400 cm^{-1}, the characteristic peak of the hydroxyl group ν(OH) is recorded, overlapped with N–H stretch at 3278 cm^{-1}. At 1657 and 1594 cm^{-1} appear the characteristic peaks of CS with high intensity that correspond to the vibration

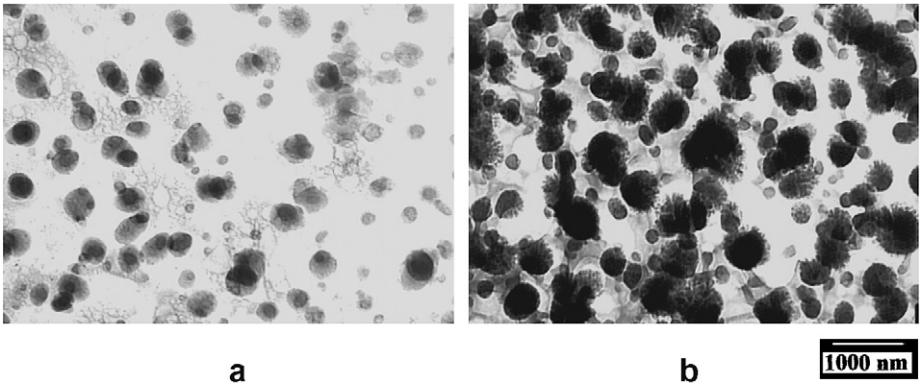

Fig. 2. TEM photographs of (a) CS/Dorzo nanoparticles (90/10 w/w) and (b) CS/Prami nanoparticles (50/50 w/w).

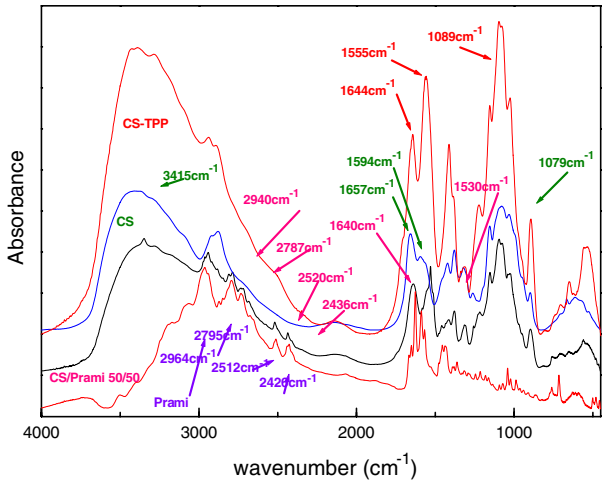

Fig. 3. FT-IR spectra of CS, CS/TPP nanoparticles, Prami and nanoparticles CS/Pram 50/50 w/w.

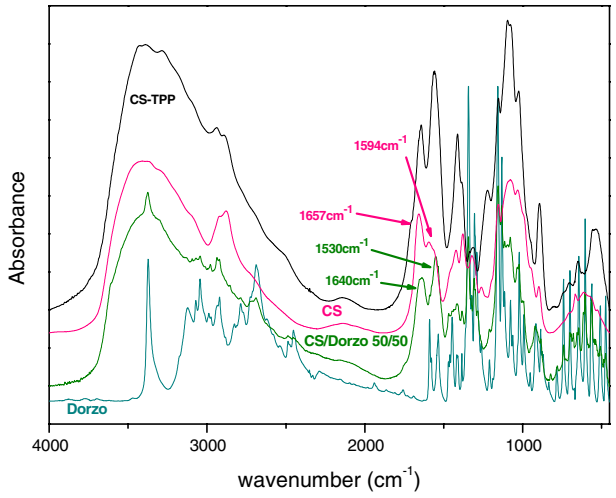

Fig. 4. FT-IR spectra of CS, Dorzo and nanoparticles CS/Dorzo 50/50 w/w.

of amide I band and amide II band, respectively. At 1322 cm^{-1} is recorded the C–N stretch and finally at 1079 cm^{-1} appears the peak of C–O stretch group. In the spectrum of CS nanoparticles prepared with TPP addition without any drug, the amino group absorption is shifted at 1640 cm^{-1}, which is an indication that these groups interacted with TPP creating ionic bonds. These interactions reduce CS solubility and are responsible for CS separation from the solution in the form of nanoparticles. Furthermore, the absorption band at 1594 cm^{-1} that was assigned to the amino groups of CS with high deacetylation degree is shifted to 1530 cm^{-1} after the conjugation reaction with TPP, indicating the formation of new amide bonds by ionic interactions with TPP. Hydroxyl groups have a broad absorption with maximum at 3416 cm^{-1}, which remains almost at the same position in the formed nanoparticles.

Many characteristic peak absorbances of Prami were shifted to different wavenumbers when it was entrapped in the nanoparticles (Fig. 4), indicating the existence of strong interaction between Prami and nanoparticles' matrix. Shifts to lower wavenumbers are recorded in the peaks located at 2512 and 2426 cm^{-1}, which in nanoparticles appear at 2520 and 2436 cm^{-1}, respectively. These peaks are attributed to the tertiary amine hydrochloride stretch of Prami. Small shifts are recorded for the peaks located at 3069 and 3171 cm^{-1} of the primary and secondary amino groups of the drug at new wavenumbers 3076 and 3172 cm^{-1}, respectively. Some other differences are recorded at the wavenumbers 1642 cm^{-1} that is shifted to 1638 and at 1557 cm^{-1}, which is shifted to 1540 cm^{-1}. A second peak at 1529 cm^{-1} was recorded in the spectrum of Prami/CS nanoparticles. All these shifts in the IR spectrum of encapsulated Prami indicate that strong interactions are taking place between Prami and CS/TPP matrix.

When Dorzo was entrapped in CS nanoparticles, no significant changes in the IR spectrum of the drug occurred (Fig. 5). Dorzo has a strong absorbance at 3372 cm^{-1} attributed to the primary amino groups. This peak in nanoparticles is slightly moved at 3374 cm^{-1}, which is a clear indication that the Dorzo interactions with CS are very poor. Furthermore, Dorzo has two additional strong peaks at 1589 and 1534 cm^{-1}. Unfortunately, these peaks are overlapped from the strong absorption band of CS, recorded at exactly the same positions in the nanoparticles, and thus it is not possible to extract any further conclusion from there. However, in a recent study encapsulating acetaminophen drug into CS particles, it was reported that interactions between the >C═O group of acetaminophen and CS are taking place and not between the >NH group and CS reactive groups (Takahashi, Chen, Okamoto, & Danjo, 2005). So, it seems in our case that the amino groups of Dorzo can not create strong interactions with the amide or with hydroxyl groups of CS.

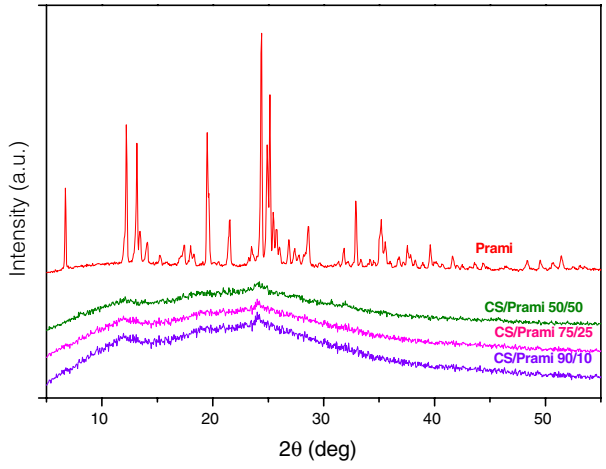

Fig. 5. WAXD patterns of Prami and drug-loaded CS nanoparticles containing different amounts of Prami.

3.3. Physical state of encapsulated drugs

In order to identify the physical state of the drugs incorporated in CS nanoparticles, wide angle X-Ray diffractometry (WAXD) was used and the patterns of pure drugs and drug-loaded CS nanoparticles were obtained. In the WAXD pattern of pure Prami, significant diffraction peaks can be observed at $2\theta = 6.7°$, 12.2°, 13.15°, 19.5°, 21.5°, 24.35°, 24.9°, 25.15°, 28.6°, 32.9° and 35.2°, characteristic of the crystalline form of the drug. To the contrary, no Prami crystallinity could be detected in the nanoparticles, irrespective of the Prami/CS ratio (Fig. 6). In the WAXD patterns of the Prami/CS nanoparticles, the broad amorphous hallow predominated while the small peaks at $2\theta = 12.09°$, 18.65° and 24.26° can be attributed to the crystalline structure of CS. Prami probably formed a molecular dispersion or an amorphous nanodispersion within the CS matrix of the nanoparticles (Gupta & Bansal, 2005; Kausbal, Gupta, & Bansal, 2004). The IR spectrum of encapsulated Prami (Fig. 4) indicated that strong interactions were taking place between Prami and CS/TPP matrix, which were responsible for the type of Prami dispersion in the nanoparticles. Such dispersions are very difficult to form in the case that a crystalline polymer is used as drug matrix, since the polymer crystals can act as nucleating agents for drug crystallization (Papageorgiou et al., 2006). However, amorphous dispersions are usually the case when amorphous polymers are used as drug carriers (Karavas, Georgarakis, & Bikiaris, 2006a) and drug amorphization can be attributed to the existence of potent interactions between the drug and the carrier.

On the contrary to what was observed with Prami, Dorzo crystallizes during its entrapment in the CS nanoparticles. Characteristic peaks are recorded in the diffraction patterns of Dorzo/CS nanoparticles (Fig. 7). However, as can be seen while the initial drug exhibits peaks at $2\theta = 9.89°$, 17.25°, 20.4°, 23.1°, 28.35°, 29.5°, 32.6°, 39.6° and 42.2°, the diffraction peaks of Dorzo on its nanoparticles with CS are not recorded at the same position. Instead, new peaks at $2\theta = 9.01°$, 15.8°, 28.9°, 20.8°, 22.7°, 23.5°, 28.4° and 32.2° with low intensity could be observed. These new peaks became more obvious as the proportion of the Dorzo in the nanoparticles was increased. These new peaks were shown to belong to the polymorph structure of the drug known as Form B (Martin & Garcia, 2004). This transformation is possible when the initial crystal form in not thermodynamically stable and transforms to the most stable form during treatment in the presence of a solvent. Based on the WAXD patterns, it is concluded that Dorzo was dispersed into CS nanoparticles in the form of nanocrystalls. Probably, the low tendency of Dorzo to interact with CS and the immobilization of the drug molecules within the nanoparticles matrix favoured the crystallization of Dorzo within the nanoparticles (in contrast with Prami where the relatively strong interactions between drug and CS matrix prevented drug crystallization).

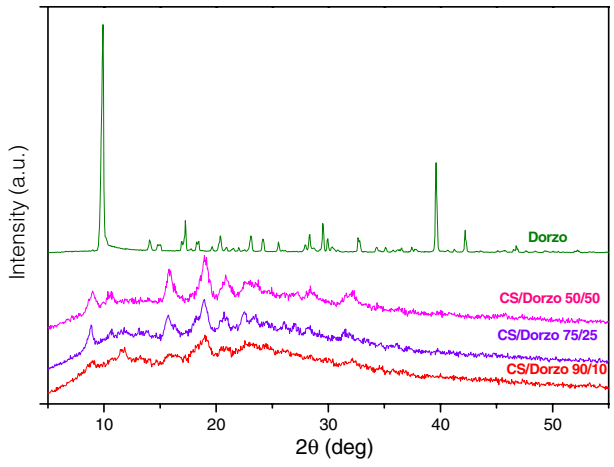

Fig. 6. WAXD patterns of the Dorzo and drug-loaded CS nanoparticles containing different amounts of drug.

The FT-IR findings (Fig. 5) may provide an explanation why Dorzo is in crystalline form in the nanoparticles. Probably, the low tendency of Dorzo to interact with CS and the immobilization of the drug molecules within the nanoparticles matrix favoured the crystallization of Dorzo within the nanoparticles. In contrast, the relatively strong interactions between Prami and CS/TPP matrix prevented the crystallization of the encapsulated Prami.

3.4. Evaluation of the physical form of Prami into CS nanoparticles

The WAXD data (Fig. 6) indicated that Prami creates a non-crystalline dispersion into the CS nanoparticles. In such dispersions, the drug could be molecularly dispersed within the nanoparticles matrix or an amorphous drug nanodispesrion is formed (Karavas, Georgarakis, Docoslis, & Bikiaris, 2007; Karavas, Georgarakis, Sigalas, Avgoustakis, & Bikiaris, 2007; Kausbal et al., 2004). Step-Scan DSC tests of the CS/Prami nanoparticles were carried out in order to examine the possible changes in the specific heat. The latter provides information with regard to the miscibility of the two components (CS/Prami) and the type of the drug dispersion. A single glass transition temperature (T_g) between the glass transitions temperatures (T_gs) of the two neat materials indicate intimate mixing between the two components in molecular level. If two T_gs are recorded, shifted at intermediate temperatures from the initial components, partial miscibility is concluded. No shift of T_gs would indicate a complete lack of miscibility. In the reversing signal thermograms, only very slight stepwise changes of the specific heat can be seen (Fig. 8). These might be associated with the glass transition of the components. However, one should be very careful since (a) at about 120–130 °C traces of water remaining in the sample evaporate, and (b) in order to accurately determine the glass transition temperature of each sample more than three runs are necessary. This is because the glass transition is characterized by a very small step in the specific heat. It should also be noted that these tests were performed using low

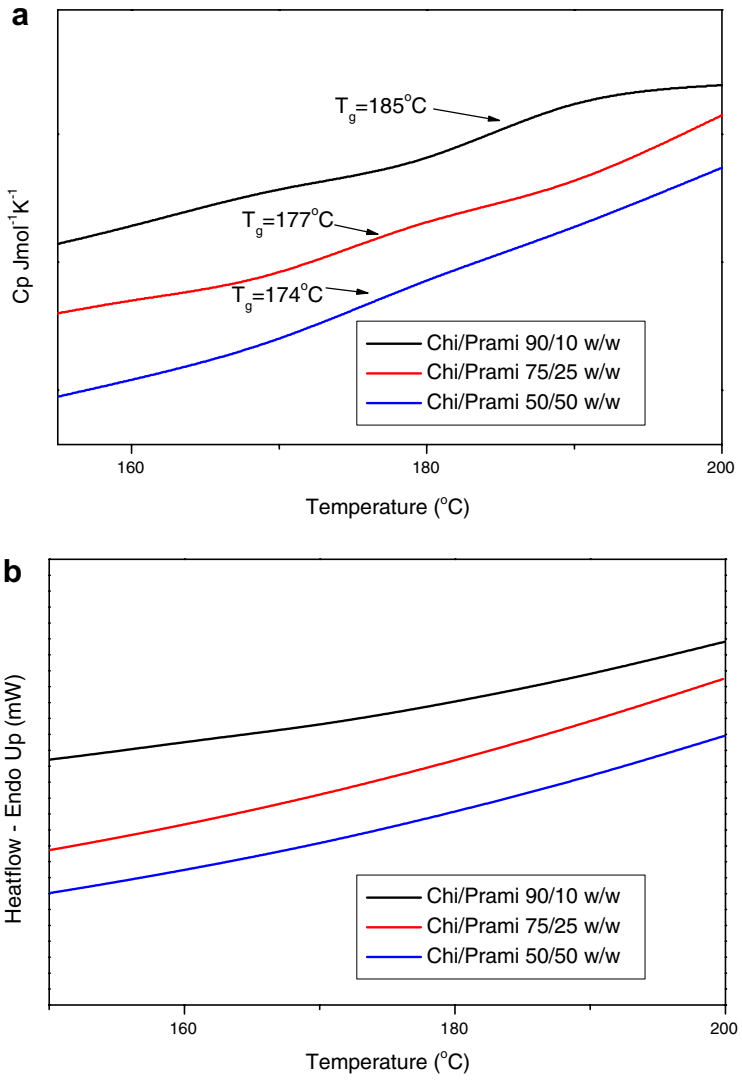

Fig. 7. Step-Scan DSC thermograms of CS/Prami nanoparticles containing different drug content. (a) Reversing signal and (b) non-reversing signal.

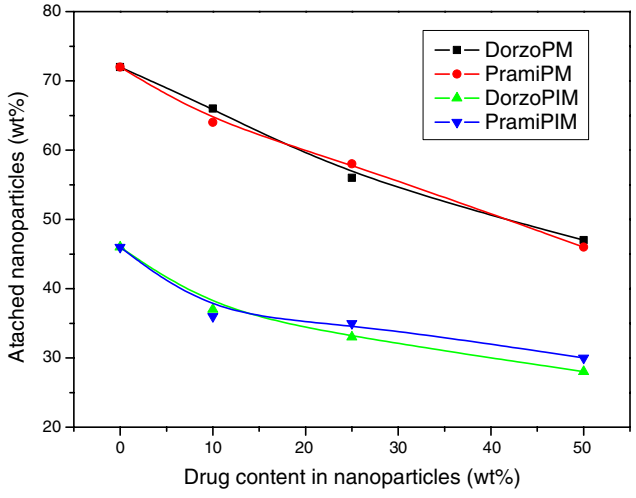

Fig. 8. Weight percent of attached nanoparticles on pig intestinal mucosa (PIM) and pig mucin bound on nanoparticles containing different amounts of dorzolamiide or Prami.

sample quantities of about 2.6 mg. Due to the low density of the samples it was not possible to use higher sample quantities. The T_g of CS nanoparticles is around 190 °C, which is much higher than the T_g of neat (uncrosslinked) CS. We have found that the T_g of neat CS is 157 °C (Karavas, Georgarakis, & Bikiaris, 2006c) and the T_g values reported in the literature for CS range between 140 and 150 °C (Dong, Ruan, Wang, Zhao, & Bi, 2004; Lazaridou & Biliaderis, 2002). Apparently after ionotropic gelation with TPP, T_g of CS was shifted at higher temperatures. Also tests for the pure Prami drug showed a step in C_p around 110–130 °C, which is evidence that the T_g of Prami lies within this temperature range. It was very difficult to melt Prami avoiding decomposition and to prepare a completely amorphous sample by quenching in liquid nitrogen. Thus partial melting to 300 °C followed by rapid cooling was preferred. With all CS/Prami nanoparticles, one glass transition temperature was recorded, which is evidence that

Prami is molecularly dispersed within the CS nanoparticles. Furthermore, in the nanoparticles contanining 10, 25 and 50 wt% Prami the glass transition is shifted (compared to cross-linked CS) to 185, 177 and 174 °C, respectively. This amorphization is in accordance with the XRD patterns (Fig. 6), which indicated that Prami is not in crystalline state (Bikiaris et al., 2005) within the nanoparticles and with the FT-IR spectra (Fig. 4) which indicated the existence of potent interactions between Prami and CS in the nanoparticles.

3.5. Estimation of nanoparticles mucoadhesive strength

The estimation of mucoadhesive strength is relatively easy in neat polymers in the form of film and several methods have been reported which produce accurate results for the mucoadhesive forces in polymer films (Karavas, Georgarakis, & Bikiaris, 2006b). Similar methods with those applied for films could also be employed for microspheres (Chowdary, & Rao, 2004). However, the measurement of the mucoadhesive properties of nanoparticles is not so straightforward and only few methods for such a measurement have been reported (Bernkop-Schnürch, Weithaler, Albrecht, & Greimel, 2006; Yin et al., 2006). In this work the mucoadhesive properties of drug-loaded CS nanoparticles were evaluated using two methods: by measuring the weight fraction of nanoparticles which was adhered to pig intestinal mucosa (PIM) and by measuring the amount of pig mucin (PM) bound on nanoparticles. In Fig. 9 the attached nanoparticles to PIM as weight (%) and the PM (%weight) bound to nanoparticles are presented for CS nanoparticles containing different amounts of Prami or Dorzo drugs and drug content, as were measured by the two used methods.

Based on the data presented in Fig. 9, the neat (unloaded) CS nanoparticles have the highest mucoadhesion. As the drug content of the nanoparticles increases, the mucoadhesive strength of nanoparticles is progressively decreased. As the drug amount in the nanoparticles increases, the amount of CS available for interacting with mucin or pig mucosal decreases, leading to lower mucoadhesive strength of nanoparticles. Another factor which may contribute in the reduction of the mucoadhesive strength of nanoparticles with increasing drug content is the increase of nanoparticles size with increasing drug content of nanoparticles (Table 1). An increase in nanoparticles size would decrease nanoparticles penetration in pig mucosa and the adsorption of mucin on nanoparticles surface (as the increase in size reduces the specific surface area of the nanoparticles), leading to a decrease of the mucoadhesive strength of nanoparticles.

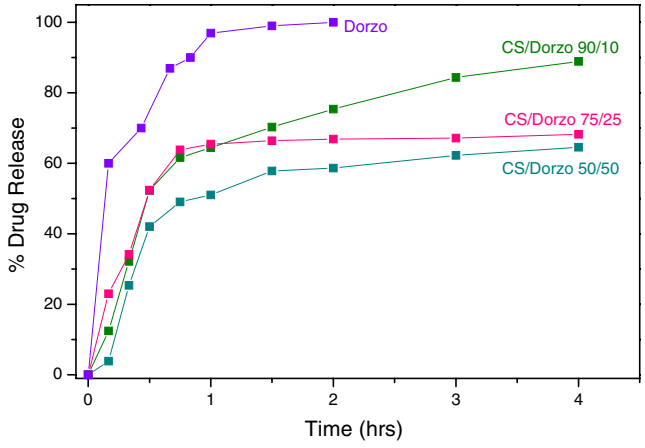

Fig. 9. In vitro drug release of CS/Dorzo nanoparticles at pH 7.4.

The type of drug (Dorzo or Prami) did not appear to affect the mucoadhesive properties of the drug-loaded CS nanoparticles. Comparing the two methods used to evaluate the mucoadhesive properties of the drug-loaded CS nanoparticles, it may be argued based on the data obtained (Fig. 9) that both methods can equally well be applied for the evaluation, in a relative sense, the mucoadhesive properties of CS nanoparticles.

3.6. In vitro drug release

The efficiency of the pharmaceutical treatment of most ocular diseases is limited by the short ocular residence time of conventional pharmaceutical forms of drugs on the ocular mucosa, due to the rapid elimination of drug from the corneal surface by the lachrymal flow. To overcome this problem, ocular administration of drugs in the form of CS nanoparticles has been proposed (Calvo, Vila-Jato, & Alonso, 1997; De Campos, Sanchez, & Alonso, 2001; Lin et al., 2007; Yuan, Li, & Yuan, 2006). CS-based systems can be used for improving the retention and biodistribution properties of drugs applied topically in the eye. Besides to its low toxicity and good ocular tolerance, CS exhibits bioadhesive and permeability-enhancing properties, which make it a unique material for the design of ocular drug delivery vehicles (Alonso & Sánchez, 2003; He, Davis, & Illum, 1998; Ludwig, 2005). In this work, Dorzo, a carbonic anhydrase inhibitor used for decreasing aqueous humour secretion in the ciliary processes of the eye, was entrapped in CS nanoparticles and the basic in vitro properties of these nanoparticles was investigated. Fig. 10 displays the release profile of Dorzo from CS nanoparticles at pH 7.4.

Comparison of the release profile of free drug (non-entrapped in nanoparticles) with the release profiles of nanoparticles makes apparent that the entrapment of Dorzo in the nanoparticles can effectively sustain Dorzo release. Sustained drug release from the nanoparticles is important, as it would allow for a prolonged residence of the drug at the surface of the eye, increasing drug bioavailability and prolonging the therapeutic effect. Dorzo release from the nanoparticles follows a biphasic pattern, characterized by an initial rapid release period (burst release) followed by a period of slower release. The burst release lasted 45 minutes, and during this period approximately 50–60% of the drug content was released from the nanoparticles. This is agreement with recent studies in

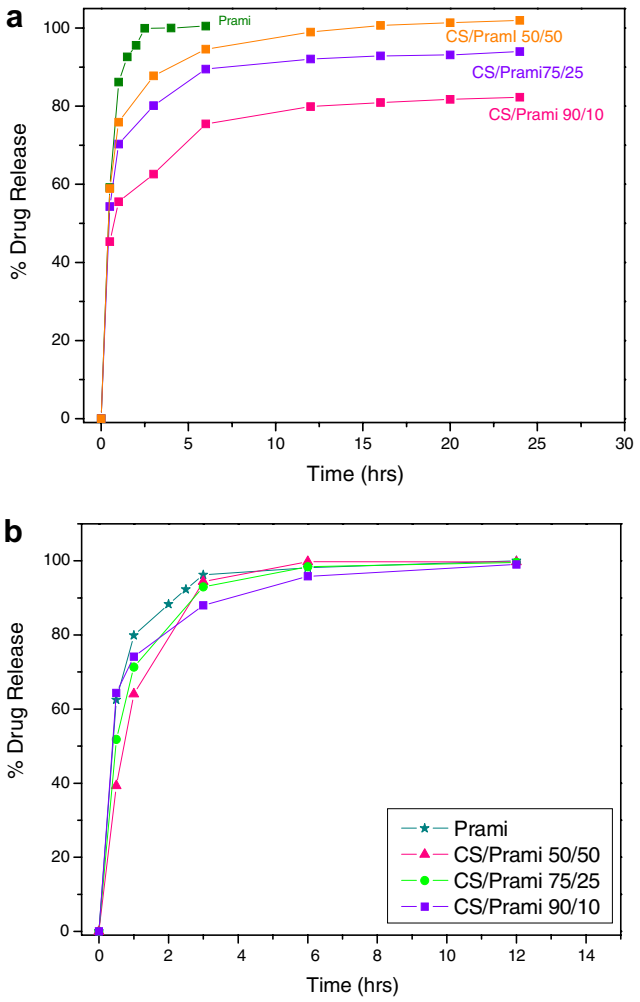

Fig. 10. Prami release from CS nanoparticles in (a) simulated intestinal fluid, pH 7.4 and (b) simulated gastric fluid, pH 1.2.

drug-loaded CS nanoparticles (Boonsongrit, Mitrevej, & Mueller, 2006) The initial fast release might be the result of the rapid dissolution of the drugs crystals located at or close to the surface of the nanoparticles. After the burst release period, the rate of release fell as the dominant release mechanism was changed to drug diffusion through the CS matrix. The overall "rate" of drug release (i.e. the fraction of drug content of the nanoparticles released at a given time) tended to become higher as the drug proportion in the nanoparticles increased. This is in agreement with a recent study of CS nanoparticles containing lysozyme (Deng et al., 2006) and is attributed to the increased porosity of the nanoparticles generated during drug dissolution.

The preparation and in vitro properties of CS nanoparticles of Prami were also investigated in this work with the long-term objective of developing an improved oral formulation of Prami. The release profiles of Prami from CS nanoparticles in bio-relevant dissolution media (simulated gastric fluid, pH 1.2 and simulated intestinal fluid, pH 7.4) are shown in Fig. 10. The release of Prami from the nanoparticles in the simulated intestinal fluid is much slower than the release of free drug in the same medium, indicating that the entrapment of Prami in CS nanoparticles can effectively control the rate of drug release (Fig. 10a). This result, and assuming that the nanoparticles will exhibit similar sustained release profiles in vivo, suggests that CS nanoparticles could be further considered as a controlled, oral drug delivery system for Prami. As in the case of Dorzo (Fig. 10), the release of Prami from the nanoparticles was biphasic. An initial fast (burst) release (about 50–75% in 1 h) occurred, which was followed by a period of much slower release. The burst release is presumably due to the fraction of drug load that is located at or close to the surface of the nanoparticles., The overall "rate" of drug release (i.e. the fraction of drug content of the nanoparticles released at a given time) increased as the drug proportion in the nanoparticles increased, mainly because the burst release was higher at increasing drug proportions (Fig. 10a). At simulated gastric fluid (pH 1.2), TPP charge is reduced (pk_{a3} and pk_{a4} of TPP are 2.3 and 6.3), respectively (Zhang et al., 2004) and the ionic interactions between CS and TPP become weaker. Thus, CS dissolves rapidly with time, allowing for a more rapid drug release from the nanoparticles in the simulated gastric fluid than in the simulated intestinal fluid (pH 7.4). The rapid Prami release from the CS nanoparticles in simulated gastric fluid is a problem with regard to the application of these nanoparticles as an oral controlled release formulation of Prami and techniques to slow down Prami release from the CS nanoparticles have to be developed. The differences in drug release rate between the nanoparticles with different drug loadingobserved in simulated intestinal fluid were no longer observed in the case of simulated gastric fluid. Given that both drugs are freely soluble in water and, thus, drug solubility was not an issue, a higher rate of drug release could have been expected from the CS/Prami nanoparticles, where the drug is molecularly dispersed, than from the CS/Dorzo nanoparticles, where the drug is in the crystalline state (WAXD data in Figs. 6 and 7). Indeed, for similar drug loading, the rate of drug release from the CS/Prami nanoparticles was a little higher than that from the CS/Dorzo nanoparticles (Fig. 10).

4. Conclusions

CS nanoparticles loaded with Dorzo or Prami were prepared and characterized. The strength of molecular interactions between the drug and the CS/TPP matrix of the nanoparticles appeared to determine the type of drug dispersion within the nanoparticles. Based on WAXD data, Dorzo was dispersed in the nanoparticles in crystalline form, probably due to the weak interaction developed between Dorzo and CS/TPP matrix as FT-IR data indicated. In contrast, WAXD and step-scan DSC data indicated that Prami formed a molecular dispersion within the nanoparticles. This was probably due to the potent interactions developed between Prami and CS/TPP matrix,

as FT-IR data revealed. The nanoparticles exhibited mucoadhesive properties, which diminished with increasing drug content. Sustained in vitro drug release was observed with the Dorzo-loaded CS nanoparticles in PBS (pH 7.4) and with the Prami-loaded CS nanoparticles in simulated intestinal fluid. The results suggest that the Dorzo-loaded CS nanoparticles and the Prami-loaded CS nanoparticles could be further evaluated for the controlled ocular delivery of Dorzo and the controlled oral delivery of Prami, respectively.

Acknowledgements

This work was funded by the Greek Ministry of Education through the postdoctoral research program EPEAEK Pythagoras I.

References

Agnihotri, S. A., Mallikarjuna, N. N., & Aminabhavi, T. M. (2004). *Journal of Controlled Release, 100*, 5.

Alonso, M. J., & Sánchez, S. A. (2003). *Journal of Pharmacy and Pharmacology, 55*, 1451.

Alonso, M. J., Calvo, P., Remunan, C., Vila-Jato, J. L. (2001). European Patent 0860166 A1.

Aktas, Y., Andrieux, K., Alonso, M. J., Calvo, P., Gürsoy, R. N., Couvreur, P., et al. (2005). *International Journal of Pharmaceutics, 298*, 378.

Bernkop-Schnürch, A., Weithaler, A., Albrecht, K., & Greimel, A. (2006). *International Journal of Pharmaceutics, 317*, 76.

Bikiaris, D., Papageorgiou, G. Z., Stergiou, A., Pavlidou, E., Karavas, E., Kanaze, F., et al. (2005). *Thermochimica Acta, 439*, 58.

Bodmeier, R., Chen, H., & Paeratakul, O. (1989). *Pharmaceutical Research, 6*, 413.

Boonsongrit, Y., Mitrevej, A., & Mueller, B. W. (2006). *European Journal of Pharmaceutics and Biopharmaceutics, 62*, 267.

Calvo, P., Vila-Jato, J. L., & Alonso, M. J. (1997). *International Journal of Pharmaceutics, 53*, 41.

Calvo, P., Remunan-Lopez, C., Vila-Jato, J. L., & Alonso, M. J. (1997). *Journal of Applied Polymer Science, 63*, 125.

Chowdary, K. P. R., & Rao, Y. S. (2004). *Biological and Pharmaceutical Bulletin, 27*, 1717.

Cui, F., Qian, F., & Yin, C. (2006). *International Journal of Pharmaceutics, 316*, 154.

De Campos, A. M., Sanchez, A., & Alonso, M. J. (2001). *International Journal of Pharmaceutics, 224*, 159.

Deng, Q. Y., Zhou, C. R., & Luo, B. H. (2006). *Pharmaceutical Biology, 44*, 336.

Dodane, V., & Vilivalam, D. (1998). *Pharmaceutical Science and Technology Today, 16*, 246.

Dong, Y., Ruan, Y., Wang, H., Zhao, Y., & Bi, D. (2004). *Journal of Applied Polymer Science, 93*, 1553.

Fernandez-Urrusuno, R., Calvo, P., Remunan-Lopez, C., Vila-Jato, J. L., & Alonso, M. J. (1999). *Pharmaceutical Research, 16*, 1576.

Gupta, P., & Bansal, A. K. (2005). *AAPS Pharmaceutical Science Technology, 6*, E223–E230.

Hirano, S., & Noishiki, Y. (1985). *Journal of Biomedical Materials Research, 19*, 413.

He, P., Davis, S. S., & Illum, L. (1998). *International Journal of Pharmaceutics, 166*, 75.

Illum, L. (1998). *Pharmaceutical Research, 15*, 1326.

Illum, L. (2007). *Journal of Pharmaceutical Sciences, 96*, 473.

Janes, K. A., Calvo, P., & Alonso, M. J. (2001). *Advanced Drug Delivery Reviews, 47*, 83.

Janes, K. A., & Alonso, M. J. (2003). *Journal of Applied Polymer Science, 88*, 2769.

Kamath, K. R., & Park, K. (1994). In J. Swric & J. C. Boylan (Eds.). *Encyclopedia of Pharmaceutical Technology* (Vol. 10, pp. 133). New York: Marcel Dekker.

Karavas, E., Georgarakis, E., & Bikiaris, D. (2006a). *International Journal of Pharmaceutics, 313*, 189.

Karavas, E., Georgarakis, E., & Bikiaris, D. (2006b). *European Journal of Pharmaceutics and Biopharmaceutics, 64*, 115.

Karavas, E., Georgarakis, E., & Bikiaris, D. (2006c). *Journal of Thermal Analysis and Calorimetry, 84*, 125.

Karavas, E., Georgarakis, E., Sigalas, M. P., Avgoustakis, K., & Bikiaris, D. (2007a). *European Journal of Pharmaceutics and Biopharmaceutics, 66*, 334.

Karavas, E., Georgarakis, E., Docoslis, A., & Bikiaris, D. (2007b). *International Journal of Pharmaceutics, 340*, 76.

Kausbal, A. M., Gupta, P., & Bansal, A. K. (2004). *Critical Review Therapeutically Drug Carrier Systems, 21*, 133.

Kim, D. G., Jeong, Y. I., Choi, C., Roh, S. H., Kang, S. K., Jang, M. K., et al. (2006). *International Journal of Pharmaceutics, 319*, 130.

Kotez, A. F., de Leeuw, B. J., Lueben, H. L., de Boer, A. G., Verhoef, J. C., & Junginger, H. E. (1997). *International Journal of Pharmaceutics, 159*, 243.

Kumar, M. N. V. R., Muzzarelli, R. A. A., Muzzarelli, C., Sashiwa, H., & Domb, A. J. (2004). *Chemical Reviews, 104*, 6017.

Lazaridou, A., & Biliaderis, C. G. (2002). *Carbohydrate Polymers, 48*, 179.

Lavelle, E. (2000). *Expert Opinion on Therapeutic Patents, 10*, 179.

Lin, H. R., Yu, S. P., Kuo, C. J., Kao, H. J., Lo, Y. L., & Lin, Y. J. (2007). *Journal of Biomaterials Science, Polymer Edition, 18*, 205.

Ludwig, A. (2005). *Advanced Drug Delivery Reviews, 57*, 1595.

Martin, J. J., Garcia L. P. (2004). WO 2004/016620 A1.

Pan, Y., Li, Y. J., Zhao, H. Y., Zheng, J. M., Xu, H., Wei, G., et al. . *International Journal of Pharmaceutics, 349*, 139–147.

Papageorgiou, G. Z., Bikiaris, D., Karavas, E., Politis, S., Docoslis, A., Yong, P., et al. (2006). *The AAPS Journal, 8*, E623–F631.

Paul, W., & Sharma, C. (2000). *S.T.P Pharma Science, 10*, 5–22.

Prabaharan, M., & Mano, J. F. (2005). *Drug Delivery, 12*, 41.

Prego, C., Garcia, M., Torres, D., & Alonso, M. J. (2005). *Journal of Controlled Release, 101*, 151.

Takahashi, H., Chen, R., Okamoto, H., & Danjo, K. (2005). *Chemical and Pharmaceutical Bulletin, 53*, 37.

Takeuchi, H., Yamamoto, H., Niwa, T., Hino, T., & Kawashima, Y. . *Pharmaceutical Research, 13*, 896.

Van der Lubben, I. M., Verhoef, J. C., Borchard, G., & Junginer, H. E. . *Advanced Drug Delivery Reviews, 52*, 139.

Wu, Y., Yang, W., Wang, C., Hu, J., & Fu, S. (2005). *International Journal of Pharmaceutics, 295*, 235–245.

Yin, Y., Chen, D., Qiao, M., Lu, Z., & Hu, H. (2006). *Journal of Controlled Release, 116*, 337.

Yuan, X. b., Li, H., & Yuan, Y. b. (2006). *Carbohydrate Polymers, 65*, 337.

Zhang, H., Oh, M., Allen, C., & Kumacheva, E. (2004). *Biomacromolecules, 5*, 2461.